The effects of the 2006 El Niño on tropospheric composition as revealed by data from the Tropospheric Emission Spectrometer (TES).

Jennifer A. Logan[1], Inna Megretskaia[1], Ray Nassar[1], Lee T. Murray[1], Lin Zhang[2], Kevin W. Bowman[3], Helen M. Worden[3,4], and Ming Luo[3].

[1]School of Engineering and Applied Sciences, Harvard University, Cambridge, Massachusetts, USA

[2]Department of Earth and Planetary Sciences, Harvard University, Cambridge, Massachusetts, USA

[3]Jet Propulsion Laboratory, California Institute of Technology, Pasadena, California, USA

[4]Now at Atmospheric Chemistry Division, National Center for Atmospheric Research, Boulder, Colorado, USA

Accepted for publication in *Geophys. Res. Lett.*, Dec 24, 2007.

Abstract.

The Tropospheric Emission Spectrometer (TES) is unique in providing multi-year coincident tropospheric profiles of CO, O_3 and H_2O. TES data show large differences in tropospheric CO, O_3, and H_2O over Indonesia and the eastern Indian Ocean in October-December 2006 relative to 2005. In 2006, O_3 was higher by 15-30 ppb (30-75%) while CO was higher by >80 ppb in October and November, and by ~25 ppb in December. These differences were caused by high fire emissions from Indonesia in 2006 associated with the lowest rainfall since 1997, reduced convection during the moderate El Niño, and reduced photochemical loss because of lower H_2O. The persistence of the O_3 difference into December is consistent with higher NO_x emissions from lightning in 2006. TES CO and O_3 enhancements in 2006 were larger than those observed during the weak El Niño of 2004.

1. Introduction.

El Niño Southern Oscillation (ENSO) is the most important mode of interannual variability in the tropical atmosphere, and has a strong influence on the distribution of tropospheric O_3 in the tropics. During an El Niño event, the normally warm waters and associated convection over the western Pacific and maritime continent move towards the eastern Pacific. As a result of the changes in large scale circulation and convection, O_3 increases over the maritime continent and decreases over the central Pacific [e.g., Ziemke and Chandra, 2003]. The intense El Niño in late 1997 and the associated drought led to major forest fires in Indonesia, with increases in the tropospheric column of O_3 (TCO) of 40-75% in the region [Chandra et al., 1998; Kita et al., 2000; Thompson et al., 2001]. Model studies showed that about half of the increase in O_3 was caused by changes in dynamics and the remainder by emissions of O_3 precursors from the fires [Sudo and Takahashi, 2001; Chandra et al., 2002].

Chandra et al. [2007] reported on the effects of the weak El Niño in late 2004 on tropospheric O_3 and H_2O. They derived data for the TCO from the Ozone Monitoring Instrument (OMI) and the Microwave Limb Sounder (MLS) on board the Aura satellite, and used MLS data for H_2O at 215 hPa. They found that the TCO increased by 10-20% over the maritime continent and decreased by a similar amount over the eastern Pacific, while H_2O showed similar changes of opposite sign.

There was a moderate El Niño in late 2006. Sea surface temperature anomalies in the Niño 3.4 region exceeding 0.5ºC for 3-month running means during 5 consecutive seasons are considered warm events (El Niño conditions). Anomalies were 0.9º, 1.1º, and 1.1º for the last three months of 2006, compared to 0.9º, 0.9º, and 0.8º for these months in 2004 [www.cpc.noaa.gov/products/analysis_monitoring/ensostuff/ensoyears.shtml]. Conditions were neutral in 2005.

There were large fires in Indonesia between August and November of 2006 with estimated emissions of 82 Tg CO, much higher than emissions during the same months in 2004 and 2005, 24 Tg and 14 Tg CO respectively, but much lower than emissions from the fires in 1997, 193 Tg CO [van der Werf et al., 2006; http://ess1.ess.uci.edu/~jranders].

We report here on the significant perturbations to O_3, CO, and H_2O from the 2006 Indonesian fires as seen by the Tropospheric Emission Spectrometer (TES), and compare to observations from 2005 as a neutral year; we refer to the differences for 2006-2005 as anomalies. TES provides coincident, vertically resolved, tropospheric profiles for these species. The O_3 profiles have vertical resolution of ~6 km, allowing a new perspective on the ENSO perturbation to O_3. We also compare the effects of the 2006 El Niño with those of the 2004 event.

2. Observations.

TES is a Fourier transform IR emission spectrometer [Beer et al., 2001]. It was launched on the Aura satellite in July 2004 in a sun-synchronous polar orbit with an equator crossing time of ~13:45. We use data from global surveys (GS) which consist of

16 orbits over 26 h; a new GS starts every other day. The nadir vertical profiles are spaced 1.6º apart along the orbit track and have a footprint of 5 x 8 km^2.

TES retrievals are described by Bowman et al. [2006], Clough et al. [2006], and Kulawik et al. [2006]. The O_3 and CO prior information is derived from a simulation with the MOZART model [Brasseur et al., 1998]; the prior profiles are monthly means in blocks of 10ºx60º (latitude by longitude). Prior profiles for H_2O are derived from the GEOS data assimilation analysis fields. Typical averaging kernels (AKs) are shown in Worden et al. [2007] for O_3, Luo et al. [2007] for CO, and Shephard et al. [2007] for H_2O. To ensure that the spatial structure we are analyzing is not caused by spatial patterns in the prior, we reprocess the TES profiles using a single prior (the average of those for 30ºN-30ºS), following Zhang et al. [2006].

The degrees of freedom for signal (DOFS) is a metric for the vertical information in the retrieved profile [Rodgers, 2000]. The DOFS for O_3 in the tropical troposphere is 1.5-1.7, showing that TES can distinguish between lower and upper tropospheric O_3 [Jourdain et al., 2007]. The DOFS for CO in the tropics was 1.0-1.5 after launch, but degraded to 0.6-0.8 because of changes in the instrument optical alignment. Warm up of the optical bench in November 2005 improved the TES CO signal, and average values for the DOFS doubled, with many values >2 in the tropics [Rinsland et al., 2006]. The typical DOFS for H_2O is 3-5, giving vertical resolution of ~3.5 km [Shephard et al., 2007].

We use V002 of TES data. Validation with ozonesonde data shows that TES O_3 profiles are biased high by 3-10 ppb [Nassar et al., 2007]. TES CO measurements are consistent with those of MOPITT [Luo et al., 2007a] and are within 15% of aircraft data [Luo et al., 2007b; Lopez et al., 2007]. TES H_2O profiles are within 5-15% of Vaisala radiosonde data, and within 5-40% of data from a cryogenic frostpoint hygrometer [Shephard et al., 2007].

Data quality and cloud filtering criteria used to select the TES profiles are given in the Auxiliary Material. Results are shown as monthly means binned on a grid of 4ºx5º at the 511 hPa retrieval level. As the AKs are relatively broad, the same pattern is seen over a range of several kilometers. We also show the zonal pattern for 0º -12ºS, with data binned every 15º of longitude.

3. Results.

Mixing ratios of CO in the mid-troposphere exceeded 200 ppb over Indonesia in October 2006, compared to ~110 ppb in October 2005, while those of O_3 were 45-55 ppb and 25-35 ppb respectively (see Figure 1). In September 2006, CO was generally less than 120 ppb in the regions with elevated CO in October. Over S. America, the south tropical Atlantic, and parts of southern Africa, both CO and O_3 were lower in October 2006 than in 2005.

Figure 2 shows the difference in CO, O_3, and H_2O between 2006 and 2005 for October to December. The CO anomaly over Indonesia and the eastern Indian Ocean in

October and November is >80 ppb in the center of the feature, with a maximum anomaly >125 ppb. CO is highest in the lower half of the troposphere in October and November 2006 (not shown). By December, the CO anomaly has decreased to less than ~30 ppb, and it is gone by January. We ascribe the high CO in 2006 to enhanced burning in Indonesia associated with the El Niño related drought, when fire emissions were almost six times those in 2005 in the GFED2 inventory [van der Werf et al., 2006].

Over the eastern Pacific, S. America, and the south Atlantic, CO is lower in October 2006 by 15-30 ppb, and over southern Africa it is lower by <15 ppb; differences are less than ±15 ppb in the later months. The lower CO over S. America in October 2006 is likely caused by lower fire emissions; estimates in the GFED2 inventory for August-September are ~37 Tg CO from S. America in 2006, half the amount in 2005.

The O_3 anomaly over Indonesia and the eastern Indian Ocean persists from October to December. Ozone differences are 10 ppb to >30 ppb from 15ºN to 15ºS for 3 months. As O_3 is typically very low here, this is an increase of 30-75%. The differences in Figure 2 are confirmed by ozonesonde profiles from Kuala Lumpur and Java [http://croc.gsfc.nasa.gov/shadoz]. Figure 3 shows that the anomaly is slightly larger in the lower troposphere (LT) than the upper troposphere (UT) in October; the converse is true in November. The positive O_3 anomaly is associated with a negative H_2O anomaly (Figure 2). The high O_3 over Indonesia in 2006 is likely caused by photochemical production in the LT from the high fire emissions, reduced photochemical loss (lower H_2O), and reduced convection (El Niño conditions), the same mechanisms discussed in the context of the 1997 El Niño anomaly [Chandra et al., 1998; Sudo and Takahashi, 2001]. Enhanced lightning in late 2006 compared to 2005 may also play a role as discussed below.

October shows the dipole pattern found in TCO data for 1997 and in years with minor El Niños [Chandra et al., 1998; Ziemke et al., 2002], with a negative O_3 anomaly of 10-15 ppb (15-30%) over the central Pacific. The low O_3 in October is caused by enhanced convection over the western Pacific, which mixes higher UT O_3 into the LT, a region of net photochemical loss in the remote Pacific [e.g., Schultz et al., 1999]. Maps of outgoing long-wave radiation (OLR) were used to determine regions of convection [http://www.cdc.noaa.gov/HistData]. OLR maps show that there was a much smaller region of convection in the western Pacific in November than in October 2006, which may explain the lack of a negative O_3 anomaly there in November.

Ozone is lower over Brazil and Bolivia by 10-30 ppb in October 2006 (likely related to lower fire emissions), and is higher in December by 5-15 ppb. Ozone is 15-30 ppb lower over equatorial Africa in December 2006. These negative anomalies are confined to the LT (Figure 3).

Water vapor is lower over Indonesia in October to December of 2006 than in 2005 by a few ppth (parts per thousand), and higher over the Pacific (Figure 2). There are not large absolute differences over the Pacific until December, although there are large relative differences (Figure S1). The changes in H_2O between 2005 and 2006 are caused by the eastward movement of convection during the El Niño year. There is much higher

H_2O (>80%) over eastern Africa and the western Indian Ocean in December 2006, which likely contributes to the lower O_3 there, because of enhanced photochemical loss. The largest relative anomaly in H_2O is located from ~600 hPa to 250 hPa at all longitudes (not shown).

The differences in values between 2004 and 2005 for CO and O_3 for November and December are smaller in magnitude and spatial extent than those between 2006 and 2005 (Figure S2). The CO anomaly in November 2004 is 25-45 ppb between Borneo and Sumatra, but is <25 ppb over the eastern Indian Ocean. Ozone is higher by 5-20 ppb in a small region over Indonesia in both months in 2004. We calculated TCO anomalies from the TES O_3 profiles over Indonesia (5°N-10°S, 90°-120°E) and found that the TES TCO anomalies for 2004-2005 are similar (within 1-2.5 DU) to those derived from OMI and MLS by Chandra et al. [2007].

4. Discussion.

We compare the TCO anomalies over Indonesia from TES for 2004 and 2006 to those derived for 1997 from total column O_3 data by Ziemke et al. [2003] in Table 1. The TCO anomaly in 2006 was smaller than that in 1997, particularly in October, but almost twice as large as that in 2004. We find that the magnitude of the TCO anomaly in October of 2004, 2006, and 1997 is related to the magnitude of CO emissions from fires in Indonesia derived by van der Werf et al. [2006], 24 Tg, 82 Tg, and 193 Tg respectively. The relatively high burning in 2006 is related to the strength of the drought, as discussed by van der Werf et al. [2007], who show that July to October of 2006 was the driest period over Indonesia since 1997.

MOPITT data show the highest CO over Indonesia in late 2006 since observations began in 2000, consistent with the relative emissions estimates in the GFED2 inventory [van der Werf et al., in preparation]. Prior to 2006, CO over Indonesia was highest in 2002, followed by 2004, both El Nino years with droughts and relatively high fires [Edwards et al., 2006].

The O_3 anomaly was almost as large in December 2006 as in November, while that for CO was much less, consistent with the fires ending in early November. The O_3 anomaly may have persisted longer than that for CO because of NO_x production by lightning when convection moved over Indonesia bringing rain. Figure 4 shows difference plots derived from the Lightning Imaging Sensor (LIS) data [Christian et al., 2003; http://thunder.msfc.nasa.gov]. There was more lightning over Indonesia in November and December 2006 than in 2005 by a factor of 2-3, although there was less in October.

The tropospheric NO_2 column over Indonesia given by the SCIAMACHY and OMI instruments [Boersma et al., 2007] was higher in October-November of 2006 than in 2005 in the vicinity of fires; NO_2 was slightly elevated in December 2006 in a broader area, consistent with a larger source of NO_x from lightning.

Lower O_3 over equatorial Africa in December may also be caused by changes in convection between 2005 and 2006, although these are not necessarily ENSO related. There was a drought in eastern Africa in late 2005, and very high rainfall in 2006. More convection in 2006 would lead to more photochemical loss of O_3 in the LT, because of enhanced downward mixing of O_3 from the UT, and higher H_2O (Figure 2). There was also less lightning over much of southern Africa in late 2006 compared to 2005, except in easternmost Africa, so that NO_x emissions would be lower.

We are using simulations with the GEOS-Chem model in conjunction with TES data to explore the mechanisms responsible for differences in tropical O_3 in 2005 and 2006, including the roles of dynamics, fire emissions, and lightning. The combination of vertically resolved, co-located data for CO, O_3, and H_2O from TES offers powerful constraints on model results.

Acknowledgements.

This work was funded by grants from NASA. We acknowledge useful discussions with P. Kasibhatla about the GFED2 inventory, and thank D. B. A. Jones and K. F. Boersma for helpful comments on the paper.

References.

Adler, R.F., et al. (2003). The Version 2 Global Precipitation Climatology Project (GPCP) Monthly Precipitation Analysis (1979-Present). *J. Hydrometeor.*, *4*,1147-1167.

Beer, R., T.A. Glavich, D.M. Rider (2001), Tropospheric Emission Spectrometer for the Earth Observing System's Aura satellite, *Appl. Opt.*, *40*, 2356–2367.

Boersma, K. F., D. J. Jacob, H. J. Eskes, R. W. Pinder, J. Wang, and R. J. van der A (2007), Intercomparison of SCIAMACHY and OMI tropospheric NO_2 columns: observing the diurnal evolution of chemistry and emissions from space, *J. Geophys. Res.*, in press.

Bowman, K.W., et al. (2006), Tropospheric Emission Spectrometer: Retrieval method and error analysis, *IEEE Trans. Geosci. Remote Sens., 44(5),* 1297.

Brasseur, G.P., D.A. Hauglustaine, S. Walters, P.J. Rasch, J.F. Muller, C. Granier, X.X. Tie (1998), MOZART, a global chemical transport model for ozone and related chemical tracers 1: Model description, *J. Geophys. Res.*, *103*, 28,265–28,289.

Chandra, S., J. R. Ziemke, W. Min, and W. G. Read (1998), Effects of 1997– 1998 El Niño on tropospheric ozone and water vapor, *Geophys. Res. Lett., 25*, 3867–3870.

Chandra, S., J. R. Ziemke, P. K. Bhartia, and R. V. Martin (2002), Tropical tropospheric ozone: Implications for dynamics and biomass burning, *J. Geophys. Res., 107*(D14), 4188, doi:10.1029/2001JD000447.

Chandra, S., J. R. Ziemke, M. R. Schoeberl, L. Froidevaux, W. G. Read, P. F. Levelt, and P. K. Bhartia (2007), Effects of the 2004 El Niño on tropospheric ozone and water vapor, *Geophys. Res. Lett., 34*, L06802, doi:10.1029/2006GL028779.

Clough, S. A., et al. (2006), Forward model and Jacobians for Tropospheric Emission Spectrometer retrievals, *IEEE Trans. Geosci. Remote Sens.*, *44*(5), 1308–1323.

Edwards, D. P., G. Petron, P. C. Novelli, L. K. Emmons, J. C. Gille, and J. R. Drummond (2006) Southern Hemisphere carbon monoxide interannual variability observed by Terra/Measurement of Pollution in the Troposphere (MOPITT), *J. Geophys. Res.*, *111*, D16303, doi:10.1029/2006JD007079.

Jourdain, L., et al. (2007), Tropospheric vertical distribution of tropical Atlantic ozone observed by TES during the northern African biomass burning season, *Geophys. Res. Lett.*, *34*, L04810, doi:10.1029/ 2006GL028284.

Kulawik, S. S., et al. (2006), Calculation of altitude-dependent Tikhonov constraints for TES nadir retrievals, *IEEE Trans. Geosci. Remote Sens.*, *44*, 1334– 1342.

Lopez, J. et al. (2007), TES carbon monoxide validation during two AVE campaigns using the Argus and ALIAS instruments on NASA's WB-57F, *J. Geophys. Res.*, submitted.

Luo, M., et al. (2007a), Carbon monoxide measurements by TES and MOPITT – the influence of a priori data and instrument characteristics on nadir atmospheric species retrievals, *J. Geophys. Res.*, *112*, D09303, doi:101029/2006JD007663.

Luo, M., et al. (2007b), TES carbon monoxide validation with DACOM aircraft measurements during INTEX-B, *J. Geophys. Res.*, in press.

Nassar, R., J. A. Logan, H. M. Worden, et al. (2007), Validation of tropospheric emissions spectrometer (TES) nadir ozone profiles using ozonesonde measurements, *J. Geophys. Res.*, in press.

Osterman, G., et al. (2006), Tropospheric Emission Spectrometer TES L2 Data User's Guide, version 2.00, 1 June 2006, Jet Propulsion Laboratory, California Institute of Technology, Pasadena, CA.

Rodgers, C.D. (2000), Inverse Methods for Atmospheric Sounding: Theory and Practice, World Scientific, London.

Rinsland, C. P., et al. (2006), Nadir Measurements of carbon monoxide distributions by the Tropspheric Emission Spectrometer onboard the Aura Spacecraft: Overview of analysis approach and examples of initital results, *Geophys. Res. Lett.*, *33*, L22806, doi:10.1029/2006GL027000.

Schultz, M., et al. (1999), On the origin of tropospheric ozone and NO_x over the tropical Pacific, *J. Geophys. Res. 104*, 5829-5843.

Shephard, M. W. et al. (2007), Comparison of Tropospheric Emission Spectrometer (TES) retrievals with in situ measurements, *J. Geophys. Res*. submitted.

Sudo, K., and M. Takahashi (2001), Simulation of tropospheric ozone changes during 1997– 1998 El Niño: Meteorological impact on tropospheric photochemistry, *Geophys. Res. Lett.*, *28*, 4091– 4094.

Thompson A. M., J. C. Witte, R. D. Hudson, H. Guo, J. R. Herman and M. Fujiwara, (2001), Tropical tropospheric ozone and biomass burning, *Science*, *291*, 2128-2132.

van der Werf, G.R,, J. T. Randerson, L. Giglio, J. G. Collatz, P. Kasibhatla, and A. F. Arellano (2006), Interannual variability in global biomass burning emissions from 1997 to 2004, *Atmos. Chem. Phys. 6*, 3423-3441.

van der Werf, G.R., J. T. Randerson, L. Giglio, N. Gobron, and A. J. Dolman (2007), Climate controls on the variability of fires in the tropics and subtropics, *Glob. Biogeochem. Cycles*, submitted.
Worden, H.M., et al. (2007), Comparisons of Tropospheric Emission Spectrometer (TES) ozone profiles to ozonesondes: Methods and initial results, *J. Geophys. Res.*, 112, D03309, doi:10.1029/2006JD007258.
Zhang, L., et al. (2006), Continental outflow of ozone pollution as determined by O_3-CO correlations from the TES satellite instrument, *Geophys. Res. Lett.*, *33*, L18804, doi:10.1029/2006GL026399.
Ziemke, J. R., and S. Chandra (2003), La Nina and El Niño-induced variabilities of ozone in the tropical lower atmosphere during 1970– 2001, *Geophys. Res. Lett., 30*(3), 1142, doi:10.1029/2002GL016387.

Figure Captions.

Figure 1. TES measurements of CO (left) and O_3 (right) in ppb for October of 2005 and 2006 at the 511 hPa retrieval level.

Figure 2. The difference between 2006 and 2005 for CO (left), O_3 (center), and H_2O (right) for October to December at the 511 hPa retrieval level; CO and O_3 are in ppb, H_2O in ppth.

Figure 3. Difference between O_3 in 2006 and 2005, for 0-12ºS, for October (left) and November (right). The color scale for the O_3 difference (in ppb) is the same as that for Figure 2.

Figure 4. Percent difference in lightning flash density between 2006 and 2005, calculated from the Science Data product of LIS. The difference is shown for areas with a lightning flash density greater than 1×10^{-8} flashes sec^{-1} km^{-2} in either year.

Table 1. Tropospheric O_3 column anomaly (DU) over Indonesia in 1997, 2004, and 2006

Instrument		October	November	December
EPTOMS	1997[a]	20.3	14.4	11.4
TES	2004[b]		6.6	5.1
TES	2006[b]	11.5	11.1	10.2

Anomalies are given for the region 5°N-10°S, 90°-120°E. Data for 1996 and 1997 were obtained from http://code916.gsfc.nasa.gov/Data_services/cloud_slice/data/tropo.txt.
[a]Anomaly with respect to 1996.
[b]Anomaly with respect to 2005.

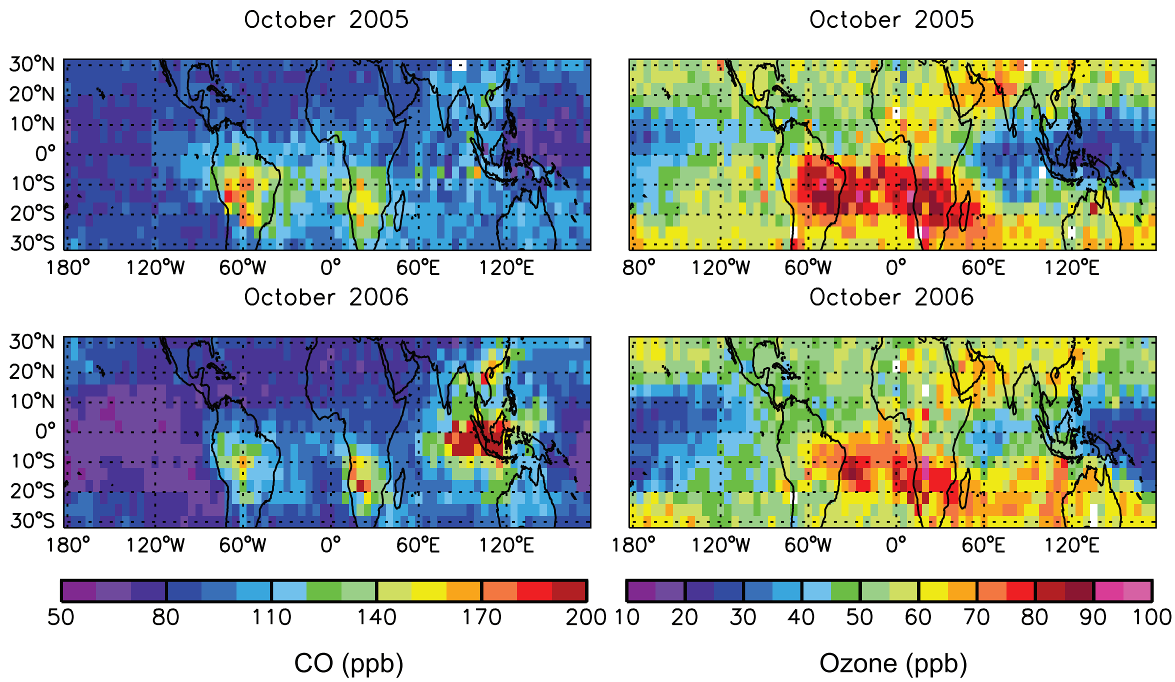

Figure 1. TES measurements of CO (left) and O_3 (right) in ppb for October of 2005 and 2006 at the 511 hPa retrieval level.

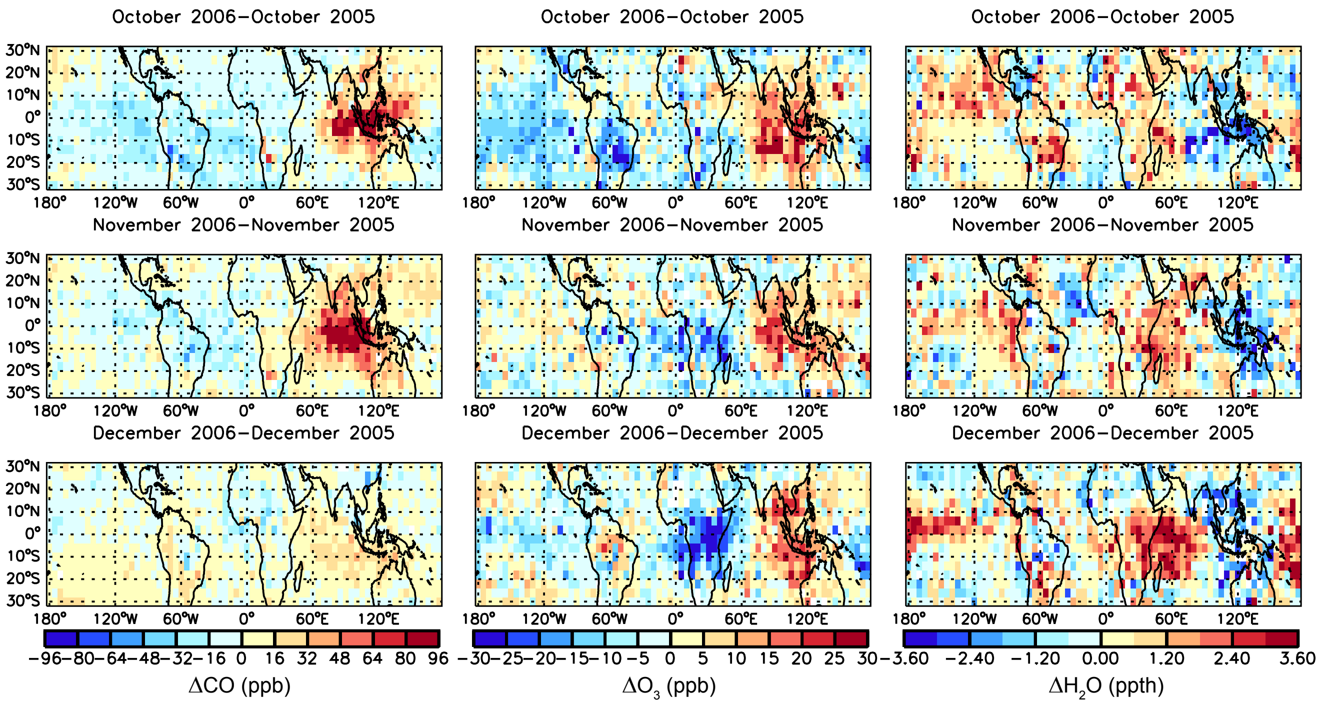

Figure 2. The difference between 2006 and 2005 for CO (left), O_3 (center), and H_2O (right) for October to December at the 511 hPa retrieval level; CO and O_3 are in ppb, H_2O in ppth.

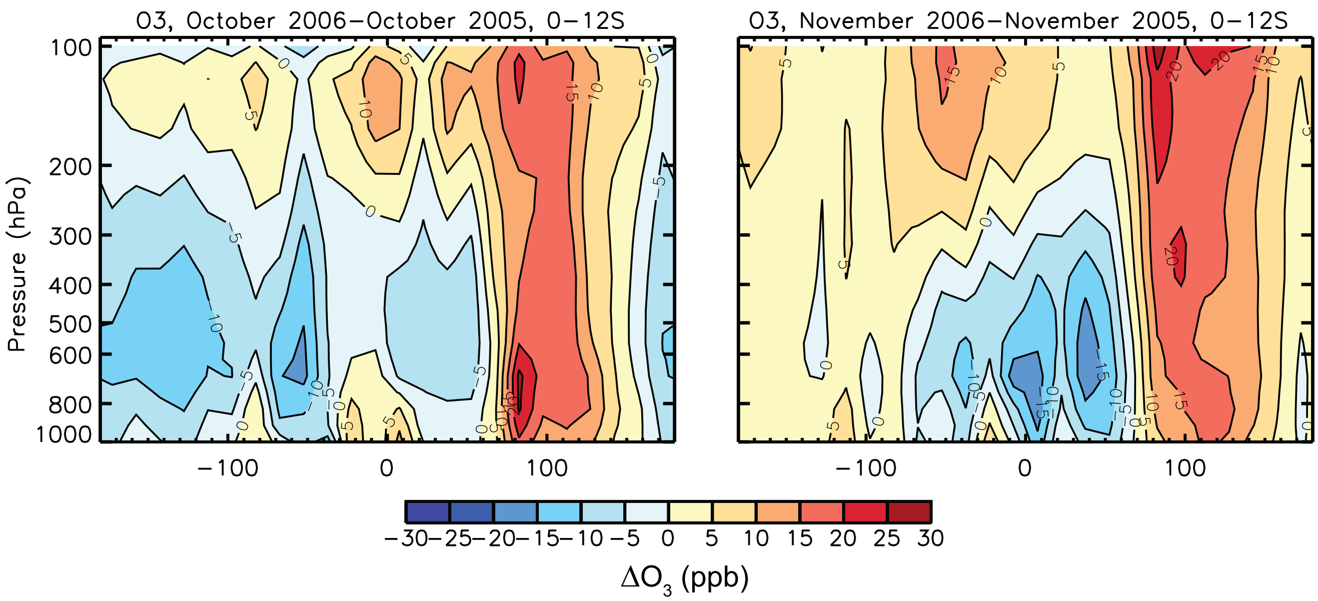

Figure 3. Difference between O_3 in 2006 and 2005, for 0-12ºS, for October (left) and November (right). The color scale for the O_3 difference (in ppb) is the same as that for Figure 2.

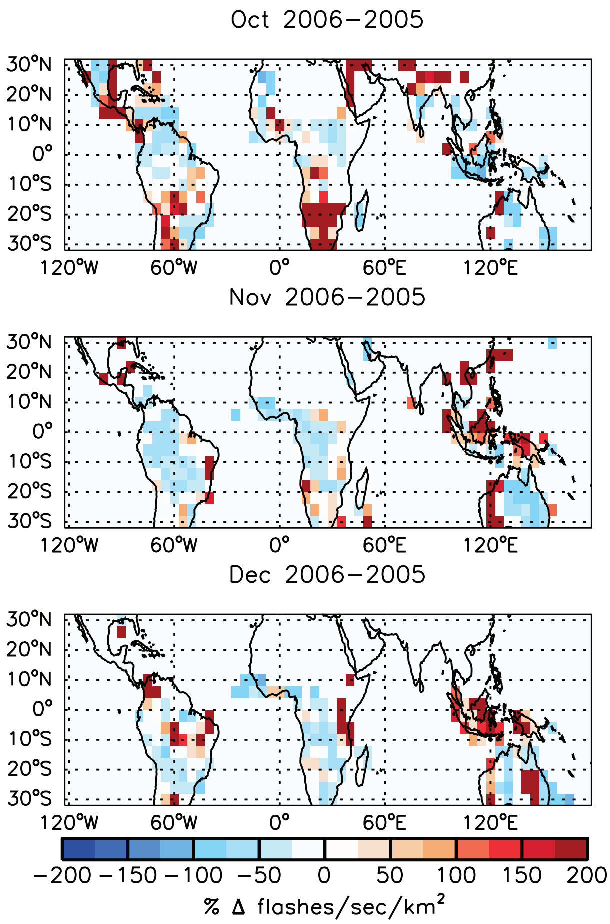

Figure 4. Percent difference in lightning flash density between 2006 and 2005, calculated from the Science Data product of LIS. The difference is shown for areas with a lightning flash density greater than 1 x 10^{-6} flashes sec^{-1} km^{-2} in either year.

Auxiliary text for Paper 2007gl031698

The effects of the 2006 El Niño on tropospheric composition as revealed by data from the Tropospheric Emission Spectrometer (TES).

Jennifer A. Logan, et al.

We selected TES data using the quality flags in *Osterman et al.* [2006]. In addition, we filter for thick clouds by excluding retrievals with a cloud top pressure less than that of the retrieval level (or 750 hPa for profile plots) and an effective optical depth >2.0, following *Nassar et al.* [2008]. For O3 and CO, we excluded retrievals with the diagonal term of the AK matrix <0.02 for 18ºN-18ºS, and <0.01 for latitudes >18º. We also excluded O3 retrievals with an emission layer near the surface with atmospheric temperatures higher than the surface temperature, as discussed in *Nassar et al.* [2008].

There were 12-16 TES nadir global surveys each month for October to December of 2005 and 2006, and for December 2004; there were only 3 global surveys in October 2005, and 11 in November, 2004. Data taken before May 21, 2005 had fewer nadir observations, which were spaced by 4.8°.

References:

Nassar, R., et al. (2008), Validation of tropospheric emission spectrometer (TES) nadir ozone profiles using ozonesonde measurements, *J. Geophys. Res.*, in press, doi:10.1029/2007JD008819.

Osterman, G., et al. (2006), Tropospheric Emission Spectrometer TES L2 Data User's Guide, version 2.00, 1 June 2006, Jet Propulsion Laboratory, California Institute of Technology, Pasadena, CA.

Supplementary figure captions.

Figure S1. The ratio of H2O in 2006 to that in 2005 for October to December at the 511 hPa retrieval level.

Figure S2. The difference in ppb between 2004 and 2005 for CO (left) and O_3 (right), for November and December at the 511 hPa retrieval level.

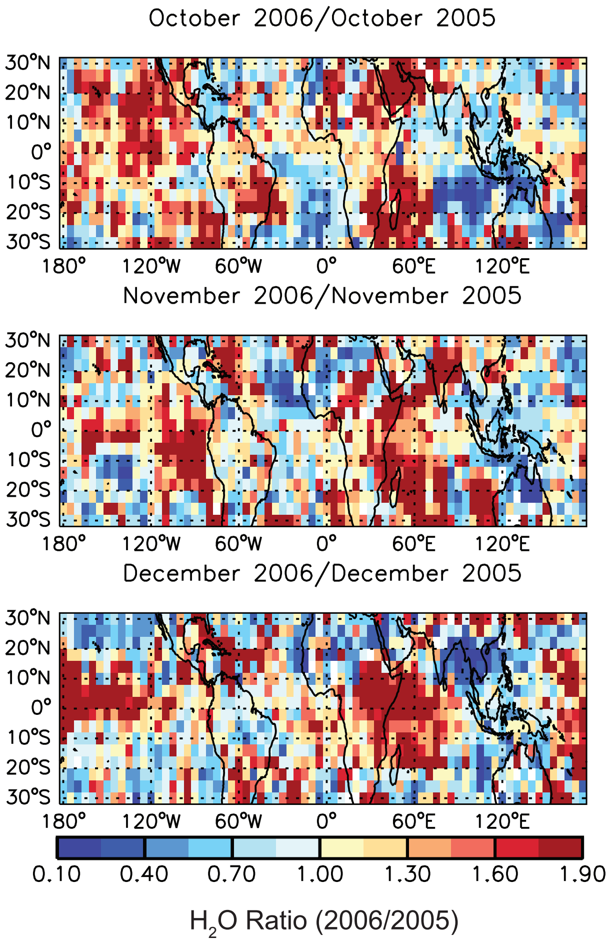
October 2006/October 2005
November 2006/November 2005
December 2006/December 2005
30°N
20°N
10°N
0°
10°S
20°S
30°S
180°
120°W
60°W
0°
60°E
120°E
0.10
0.40
0.70
1.00
1.30
1.60
1.90
H_2O Ratio (2006/2005)

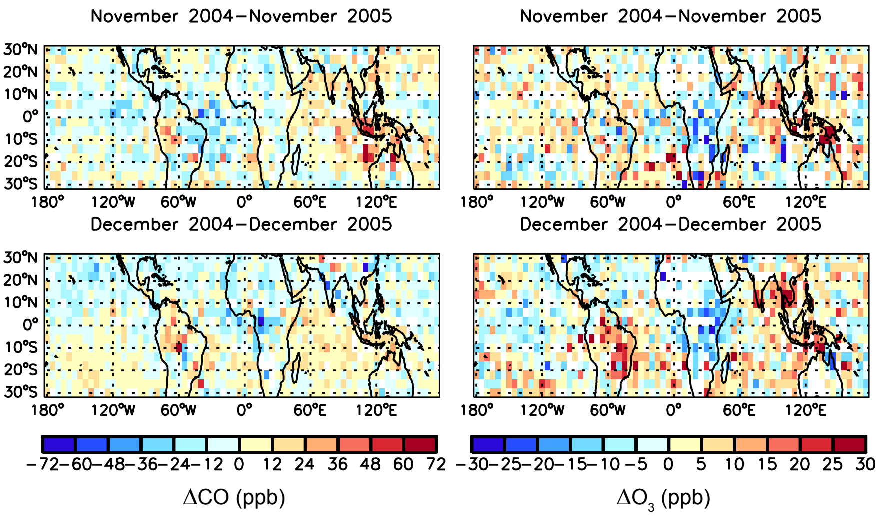

November 2004–November 2005
November 2004–November 2005
December 2004–December 2005
December 2004–December 2005
30°N
20°N
10°N
0°
10°S
20°S
30°S
180°
120°W
60°W
0°
60°E
120°E
−72 −60 −48 −36 −24 −12 0 12 24 36 48 60 72
ΔCO (ppb)
−30 −25 −20 −15 −10 −5 0 5 10 15 20 25 30
ΔO_3 (ppb)